Accepted Manuscript

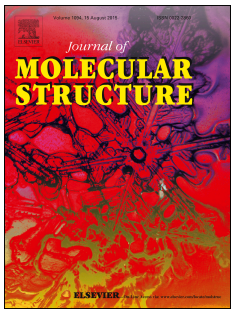

Structure investigations of Schiff bases derived from 3-amino-1H-1,2,4-triazole

Beata Kołodziej, M. Morawiak, Wojciech Schilf, Bohdan Kamieński

PII: S0022-2860(19)30151-6

DOI: https://doi.org/10.1016/j.molstruc.2019.02.027

Reference: MOLSTR 26184

To appear in: *Journal of Molecular Structure*

Received Date: 14 November 2018

Revised Date: 30 January 2019

Accepted Date: 7 February 2019

Please cite this article as: B. Kołodziej, M. Morawiak, W. Schilf, B. Kamieński, Structure investigations of Schiff bases derived from 3-amino-1H-1,2,4-triazole, *Journal of Molecular Structure* (2019), doi: https://doi.org/10.1016/j.molstruc.2019.02.027.

Graphical Abstract

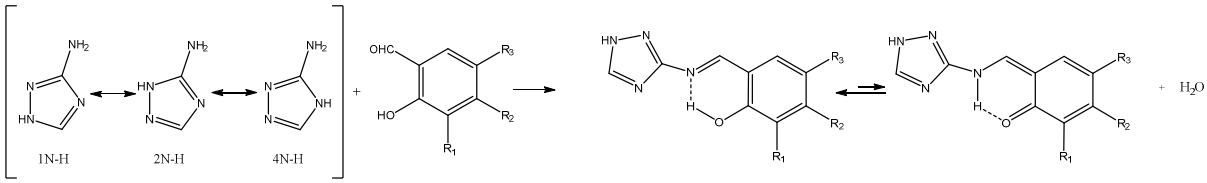

Structure investigations of Schiff bases derived from 3-amino-1H-1,2,4-triazole

Beata Kołodziej[a*], M. Morawiak[b], Wojciech Schilf[b], and Bohdan Kamieński[b,c]

a- West Pomeranian University of Technology, Szczecin; Faculty of Chemical Technology and Engineering; Department of Inorganic and Analytical Chemistry, Al. Piastów 42, 71-065 Szczecin, Poland

b- Institute of Organic Chemistry, Polish Academy of Sciences, ul. Kasprzaka 44/52, 01-224 Warsaw, Poland

c- Institute of Physical Chemistry, Polish Academy of Sciences, ul. Kasprzaka 44/52, 01-224 Warsaw, Poland

*- corresponding author

Key words

aminotriazole, Schiff bases, ^{1}H, ^{13}C, and ^{15}N NMR, FT-IR-ATR, UV-Vis, and X-ray spectroscopic methods, intramolecular hydrogen bond.

Abstract

In the present paper, twelve Schiff bases derived from 3-amino-1H-1,2,4-triazole (ATz) and various benzaldehydes, and salicylaldehydes were synthesized. The ^{1}H, ^{13}C, and ^{15}N NMR data are discussed in relation to the structure of ATz and its imine products. In addition, X-ray, ATR-FTIR, and UV-Vis analytical techniques are used for structure elucidation of ATz-based Schiff bases. It was found that the starting material, 3-amino-1H-1,2,4-triazole, exists as tautomeric mixture of three forms (Graphical Abstract) in solution, whereas in the solid state (^{13}C and ^{15}N CPMAS data) potentially tautomeric proton is located on nitrogen atom traditionally marked as N-2 (Graphical Abstract, 2N-H structure). All investigated Schiff bases derived from salicylaldehydes exist in both phases as tautomeric equilibrium mixtures, where enol-imine forms are dominated structures. The positions of those equilibria only very slightly depend on substituents in phenol ring. Generally, the contributions of keto-amine forms in the solid state are higher comparing with DMSO solutions.

Introduction

Imines derived from o-hydroxy aromatic carbonyls are of great interest because of their ability to form the asymmetric intramolecular hydrogen bond between oxygen atom of hydroxyl group and nitrogen atom of imine group [1-3]. This ability has a decisive impact on biological and thermo- or photochromic properties of o-hydroxy aromatic Schiff bases [4-7] and makes them very useful compounds in chemistry, biochemistry, medicine, and technology [8-11]. Therefore, the very important issue is determining the positions of tautomeric equilibria in these compounds. Consequently, various instrumental research techniques are used to provide insight into the structure of molecules of studied o-hydroxy Schiff bases [7, 12-13]. Determination of the position of the hydrogen atom involved in hydrogen bonding can be achieved by using a combination spectroscopic techniques (i.e., ATR-IR, UV-Vis, and heteronuclear NMR spectroscopies) and x-ray diffractometery [14-16].

Very convenient, but not always exact method of proton position estimation in intramolecular hydrogen bridge is proton NMR measurement. By this method one can obtain quick information about presence of such bonds. The signal position of proton involved in the hydrogen bonding is strongly downfield shifted to the range from 10 to even 21 ppm. Unfortunately, the chemical shift by itself does not provide reliable information about geometry of hydrogen bridge. To obtain such data it is necessary to use ^{13}C NMR data. The most valuable parameter is chemical shift of formally OH substituted aromatic carbon atom. For enol-imine structure the typical position of this signal is in the range from 155 to 165 ppm, whereas for keto-amine structure this signal is shifted close to 180 ppm [17].

Very useful in investigations of such systems is nitrogen NMR technique [18-19]. This is because of two reasons:

- high sensitivity of nitrogen chemical shift of formally imine atom (δ_{Nim}) on proton position in H-bond [20] (it is well known that δ_{Nim} for pure imine form is about -50 ÷-60 ppm and for pure enamine form is about -220 ÷-240 ppm),
- low sensitivity of δ_{Nim} on the substitution effects connected with different substituents in salicylaldehyde unit [21-22].

Infrared spectroscopy is a method very readily used in order to confirm the existence of an imine group in Schiff bases [23]. In the case of simple imines there is no problem in assigning the bandwidth of the binding site. However, if the imine has in its structure additional groups (for example –COOH, -C=O) giving bands in the same area, this task becomes more difficult [24].

UV-Vis spectroscopy is recognized as a very good and sensitive method to determining the tautomeric equilibria of o-hydroxy Schiff bases in various solvents [25-26]. Generally, if the compound exists mainly in enol-imine form, in UV-Vis spectrum strong band below 400 nm is expected. The position of the band in the spectrum above 400 nm suggests shifting of tautomeric equilibrium to keto-amine form [27]. UV-Vis spectroscopy in the solid state (UV-Vis-DR) is much less common than in solution, and there are few works about analysis of Schiff bases by this method [28-29]. One of the reason of rare use of this method is probably the shape of the obtained spectra, where bands are very often widened and overlapping.

In the present paper we describe synthesis and instrumental analysis of twelve (three new) Schiff bases derived from 3-amino-1H-1,2,4-triazole (Amitrole, ATz), which is a heterocyclic primary amine having in the five-membered ring three nitrogen atoms potentially involved in tautomeric exchange (Fig.1) [4, 30].

Fig.1

This amine is a very good substrate for synthesis of biologically active compounds. It is well known that 1,2,4-triazole ring (blue part in Fig.1) has a strong interaction with heme iron, and the substituted triazoles are potent for the inhibition of ergosterol, which is the main constituent of fungal cell membrane [4, 31]. Furthermore, Amitrole inhibits production of imidazoleglycerol-phosphate dehydratase (gene HIS3) in Saccharomyces cerevisiae [30, 32]. Triazoles are considered as good corrosion inhibitors due to the presence of three nitrogen atoms acting as adsorption centers and due to their environmental acceptability [33]. A literature survey revealed that triazolyl Schiff bases are of great interest in medicinal chemistry because of their capability to form stable intermediates which are connected with diverse biological activity [4].

Experimental

Synthesis of Schiff bases

All compounds were synthesized by standard procedure [34] slightly modified for the present reaction.

To a methanolic solution of ATz (2.3 mmol) a methanolic solution of suitable aldehyde (2.3 mmol) was added. The mixture was stirred and refluxed for 30 min, allowed to cool to ambient temperature and was left undisturbed for 24 hours.

The resulting precipitate was filtered off in a water pump filter kit, washed with cold methanol and air dried.

The authenticity and purity of obtained compounds were examined by proton NMR measurements.

For two imines suitable for X-ray measurements single crystals have been obtained.

NMR measurements

The all NMR experiments in DMSO-d6 solution were performed on Varian-Agilent 600 MHz VNMRS instrument using 5 mm inverse probehead equipped with Z-gradient coil. The chemical shifts assignment in proton and carbon spectra was done on the base of 2D experiments (GCOSY, GHSQC and GHMBC). The acquisition of data and spectra processing was done using standard Agilent software. Internal TMS was applied as the standard compound for chemical shifts of proton and carbon spectra. For nitrogen-15 experiments (2D GHMBC), external nitromethane was applied as the chemical shift standard (0 ppm).

The solid state NMR spectra were done using Bruker Avance 500 MHz spectrometer equipped with 4mm CPMAS broadband probehead. The standard experimental parameters for carbon CPMAS spectra were: spectral width 31 kHz, acquisition time 20 ms, contact time 2 ms, spin rate 12 kHz. The short contact time experiments (SCT) were applied to differentiate protonated and quaternary carbon atoms. For those experiments contact time equal 40 μs was applied. Originally, the carbon solid state spectra were referenced to the glycine sample and then the obtained chemical shifts values were recalculated to TMS scale. For nitrogen spectra similar procedure was applied to recalculate chemical shifts values to nitromethane as the standard. For nitrogen CPMAS experiments the following acquisition parameters were applied: spectral width 25 kHz, acquisition time 20 ms, spin rate 6-12 kHz, contact time for spin-lock 4ms, relaxation delay 10 to 120 s depending on relaxation condition for particular sample, the values parameter were estimated from carbon measurement. For SCT nitrogen measurements the contact time was reduced to 0.1 ms.

X-ray structure analysis

Crystals of two of ATz-based Schiff bases were obtained from methanol: colourless crystals of 4BrbenzATz, and light yellow crystals of 4BrsalATz. Crystal data for these compounds were collected at room temperature, on Bruker X8 APEXII diffractometer using Cu-Kα radiation (λ = 1.54178 Å) (Table 1 (Suppl. Mat.)). Frames were integrated with the Bruker SAINT [35] software package using a narrow-frame algorithm. The structure was

solved and refined using the Bruker SHELXTL Software Package [36]. Data were corrected for absorption effects using the face-indexed numerical method (SADABS) [37]. Hydroxyl group hydrogens and N-hydrogen were found from the difference electron density maps and refined with an anisotropic thermal motion model. Other hydrogen atoms were placed in calculated positions and refined as riding on their parent atoms with U_{iso} = 1.2 Ueq. The structure was solved by direct methods SHELXS-2014 [38] and refined with full-matrix least-squares calculations on F^2 using SHELX-2014 [38]. All non-hydrogen atoms were refined anisotropically.

Crystallographic data have been deposited at the Cambridge Crystallographic Data Centre, 12 Union Road, 129 Cambridge CB2 1EZ, UK, and copies can be obtained on request, free of charge, by quoting the publication citation and the deposition number CCDC 1867614 for 4BrbenzATz and CCDC 1867615 for 4BrsalATz.

ATR-FTIR measurements

ATR-FTIR spectra were recorded on a Bruker Alpha Fourier Transform IR (FTIR) spectrometer equipped with a platinum ATR single reflection diamond-sampling module (Bruker Optics).

The infrared spectra were collected as an average of 24 scans per sample between the wavenumber range of 4000–360 cm^{-1} at a resolution of 4 cm^{-1}, controlled by Optics User Software (OPUS) version 7.5 (Bruker Optics). Air was used as reference background spectra. The ATR diamond surface was cleaned with acetone before each sample was scanned.

UV-Vis measurements

a) in solution

UV-Vis spectra were recorded at room temperature on the double-beam UV-Vis absorption spectrometer, Jasco V-670, using a 1.0 cm matched silica cells. The UV-Vis spectra measured in $CHCl_3$, CH_3CN, and $(CH_3)_2SO$ solutions were collected in the wavelength range of 190-800 nm.

b) in the solid state (UV-Vis-DR measurements)

Diffuse reflectance (DR) spectra were recorded on a Jasco V-670 spectrometer equipped with an integrating sphere accessory at room temperature.

The powdered compounds were each packed into the sample holder, which was placed in the next step in the sample space of the instrument.

The UV-Vis-DR spectra were collected between the wavelength range from 190 to 800 nm, controlled by JASCO Spectra Analysis. Spectralon was used as a reference background spectra. Cuvette was cleaned with acetone before each sample was scanned.

Results and discussion

1. NMR spectroscopy

The structures and atom numbering in investigated ATz-based Schiff bases are presented in Fig.2, and the full set NMR measurements results in DMSO-d6 solution are collected in Table 2.

Fig.2

Table 2

The proton and carbon atoms signals assignment has been done on the base of both homo- and heteronuclear 2D spectra (COSY, GHSQC and GHMBC). The differentiation of carbon signals (C-3' and C-5') of triazolyl ring was done applying one-bond correlation with protons in H-5' position (Fig.2). This correlation was observed for some derivatives, where those proton signals were relatively sharp (typical chemical shift of H-5' signal close to 8.5 ppm). Generally the C-3' signals were found by correlation with H-7 proton signals. Unfortunately, due to dynamic character of triazolyl ring, which causes severe broadening of both proton signals in triazolyl ring (H-1' and H-5'), we could not detect in DMSO-d6 solution any nitrogen atoms signals from this part of molecules. We could measure only N_{im} signals obtained by correlation with very characteristic H-7 proton signals. The positions of OH and NH protons were defined by comparison of salicylaldehydes derivatives spectra with those of benzaldehydes derivatives, where OH signals do not exist. The carbon signals assignment in CPMAS spectra has been done by comparison of regular ^{13}C solid state spectra with short contact time SCT experiments (only protonated carbon signals are present), and by analysis of characteristic position of signals in both solution (Table 2) and solid state (Table 3) spectra. The nitrogen signals assignment in solid state spectra has been performed using SCT experiments to verify positions of N-1' signals. In all cases the upfield signals close to -170 ppm were detected as NH signals. To decide how to assign those signals to proper positions in triazolyl ring it is necessary to analyze nitrogen chemical shifts of aminotriazole and some of its methyl derivatives, where tautomeric equilibrium is eliminated (Fig.3).

Fig.3

If we compare the nitrogen chemical shifts of three methyl derivatives (Fig.3, I) [39-40], where tautomeric exchange is eliminated, with those obtained for ATz in the solid state, we can decide that in this phase hydrogen atom in ATz is located on nitrogen atom close to NH_2 group (Fig.3, II), similar to A structure (Fig.3, IA). In nitrogen CPMAS spectra of o-hydroxy Schiff bases the only one NH signal was found in each compound. In all discussed cases the NH signals are located in relatively narrow spectral range close to -170 ppm. It means that triazolyl part in studied imines does not correspond to the A structure. The chemical shifts patterns observed for all Schiff bases in the solid state (Table 3) are very similar to the B structure, which is postulated for those compounds. It means that we need to assign them to different ring position comparing with ATz, so we can assume that in all salicylaldehyde derivatives in the solid state the triazolyl ring has structure similar to compound B. Consequently, the remaining signals from lowfield region (close to -100 ppm) should be assigned to the atoms from –N-N- moiety and finally the signals from -150 to -170 ppm range should be assigned to N-4’ position. Unfortunately, in the lowfield range (-100 ÷ -120 ppm) the imine nitrogen signals can be located making exact signal assignment impossible.

For imines obtained from ATz and salicyldehydes two major structure problems have to be solved. The first problem is possible tautomeric equilibrium in triazolyl rings and the second one is presence or not of the intramolecular hydrogen bonds between OH hydrogen atoms and formally imine nitrogen atoms. If such bonds are present it is necessary to determine the position of hydrogen atom in such bridge.

The tautomeric equilibrium in triazolyl ring can be detected by analysis of dynamic broadening of appropriate proton and carbon signals. In all investigated imines the very similar carbon chemical shifts in C-3’ and C-5’positions respectively were measured in both phases. It means that in DMSO-d6 solution and in the solid state the same tautomeric equilibria exist. Since we excluded location of hydrogen atom in position 4’ in solid state, consequently in DMSO-d6 we should do the same. It reduces tautomeric equilibrium process to exchange proton position between N-1’ and N-2’ site. In all imines we observed single broadened signals (position 3’ and 5’) indicating fast on NMR time scale but close to coalescence exchange. The different broadening of mentioned signals of each compound informs that substituents in aromatic rings influence significantly the exchange rates of observed process but do not change the mechanism of it.

Different picture was found in proton and carbon spectra of ATz in DMSO-d6 solution: in both spectra slow on NMR time scale tautomeric exchange between

nonequivalent positions takes place. The proportion of tautomers, estimated from both spectra is close to 8:2. Unfortunately, in proton-nitrogen correlations only NH (-203.3 ppm) and NH_2 (-331.9 ppm) signals of major component were measured. The position of NH signal tells us that the major tautomer in DMSO-d6 solution has the same molecular structure as mentioned above methyl derivative A (Fig.3).

To solve the second structural problem: presence or absence of intramolecular hydrogen bonding, it is necessary to analyze the nitrogen chemical shift (N_{im}) of potentially imine nitrogen atom and carbon chemical shifts of atoms in positions 2 and 7. Some information about presence or not of this bonding can be obtained from hydrogen chemical shift of proton in the hydrogen bridge. Generally, large lowfield shift of this signal confirms presence of intramolecular hydrogen bond but does not determine exact proton position. Much better estimation of proton position in the bridge can be done by analysis of chemical shifts of N_{im} and C-2 atoms [21, 41-47]. In some cases, where the proton positions in the bridge (OH or NH form) are extremely different, position of signal of C-7 atom can give some valuable information. However, the nitrogen chemical shift seems to be the best spectral parameter for this estimation due to the highest sensitivity on proton position and the lowest sensitivity on substitution in aldehyde ring.

The proton positon in hydrogen bridge is determined by three factors: substituent in aromatic ring (all substituents, which increase the acidity of OH groups promote proton transfer from oxygen to nitrogen site), amine used for condensation (aliphatic amines shift proton to nitrogen atom comparing with aromatic amines), phase of analyzed sample (in the solid state proton is generally more shifted to nitrogen atom than in the solution). One more factor, temperature, has to be mentioned here: in elevated temperature the NH form is preferred [41-43].

Analyzing the NMR data included in Table 2 one can state, that for all salicylaldehyde derivatives studied in DMSO-d6 solution very similar structure (tautomeric equilibria where mainly OH form exists) was found. This conclusion is based on the fact that all interesting spectral parameters are located in very narrow ranges. Only in 4-OCH_3sal derivative some higher contribution of NH form should be mentioned (upfield shift of imine signal). The differences in chemical shifts of C2 atoms are less diagnostic since this parameter can be affected by aromatic ring substitution effects.

Table 3

The nitrogen chemical shifts of imine atoms in the solid state (Table 3) show that in this phase more NH form contribute in hydrogen bond structure and still the differences in the

structures between solution and solid state of all investigated salicylaldehyde derivatives are smaller comparing with simple aliphatic amine derivatives [45]. Again for 4-OCH_3sal compound nitrogen signal is the most upfield shifted in this series indicating the highest contain of NH form. The spectral data for 5-OCH_3sal and 4-Brsal derivatives are close to 4-OCH_3sal substituted compound but proton transfer processes for those compounds are not so advanced. The exact analysis of ^{15}N solid state data for remaining compounds is more complicated because the spectral ranges typical for imine atoms and N-2' atoms are overlapping. But since they are located in very narrow band, the possible error in structure estimation connected with missed assignment is small and does not change the general conclusion. The amount of signals in the solid state spectra also indicates that some polymorphic phenomena can exist. The signals of possible polymorphs are located very close one to another so one can conclude that structure of hydrogen bonds of them are very similar and observed differentiation is connected with crystal structure phenomena.

2. X-ray diffractometry

Molecular structure of compounds 4BrbenzATz and 4BrsalATz (Fig.4) show the expected bond lengths and angles, which are summarized in Table 4 (Suppl. Mat.).

Fig.4

The 4-bromobenzaldehyde derivative forms hydrogen bonds only with adjacent molecules (Fig.5), while the 4-bromosalicylaldehyde derivative, as could be predicted, additionally forms an intramolecular hydrogen bond (Fig.6). Details of the hydrogen bonds are given in Table 5.

Fig.5

Fig.6

Table 5

The bond lengths and angles in 4BrsalATz are close related to structures of 4-Bromo-2-[(E)-(1H-1,2,4-triazol-3-ylimino)methyl]phenol [48]. In the structure of the compound synthesized in the Chohan's group, hydrogen bonds with bromine (C5–H5···Br1) are not formed, which in our case determines the packing of molecules in the elementary cell (Fig. 7 (Suppl. Mat.)).

An intramolecular O1—H2···N1 hydrogen bond in 4BrsalATz, a characteristic bond for Schiff bases, leads to the formation of a S(6) six-membered ring. Additional forming of this bond causes the molecule to flatten. The dihedral angle between the plane of the 1,2,4-

triazolyl ring and the plane of the phenyl ring decreases from 19.9° for 4BrbenzATz to 4.2° for the salicylic derivative. (Fig**.** 8 (Suppl. Mat.)).

The differences between geometry of 4BrbenzATz and 4BrsalATz molecules are illustrated in Fig. 9 (Suppl. Mat.)**,** showing the overlay of molecules. The conformations of these molecules described the torsion angles φ3 = N1–C7–C1–C2 and φ6 = N2–C8–N1–C7, which are of 9.1(5)° and 10.2(5)° for 4BrbenzATz, 1.8(6)° and 1.1(6)° for 4BrsalATz, respectively.

3. ATR-FTIR spectroscopy

In analysis of infrared spectra of Schiff bases two major spectral ranges should be considered: 3500-2700 cm^{-1} and 1770 – 1550 cm^{-1}.

The first one from 3500 to 2700 cm^{-1} is usually treated as a very useful region in purity determination, as well as in hydrogen bond structure study.

In purity determination one can expect to find at least two effects:

- disappearance of the bands attributable to the N-H stretching vibrations of the primary amino group of amines (pair of two bands at about 3400 and 3300 cm^{-1} [22]),
- disappearance of the bands attributable to the C-H stretching vibrations of -CHO group of aldehydes (pair of weak bands, one at 2860-2700 cm^{-1} and the other at 2760-2700 cm^{-1} [22]).

To verify presence of hydrogen bond it is necessary to analyze the shape of appropriate band as well as its position. IR spectra of o-hydroxy aromatic imines based on heterocyclic amines in this region show broad to very broad bands with maxima in relatively broad range 3500-2700 cm-1 (3300-2700 [49]; 3500-3200 cm-1 [7]; 3200-2500 [50]). This phenomenon is treated as a proof of the hydrogen bond existence [49].

ATR-FTIR spectrum of ATz shows two bands characteristic for presence of primary amino group in the compound (Fig.10, red line, 3402 and 3322 cm^{-1}). These bands are absent in spectra of ATz-based Schiff bases (Fig.10, blue line). In the range of 3500-2700 cm^{-1} in the spectra of o-hydroxy aromatic ATz-based Schiff bases, one can observe weak broad bands (Fig.10. blue line) assigned to stretching vibrations of O-H bond engaged in intermolecular (for example HO···H-C) and intramolecular (O-H···N)hydrogen bonding. This conclusion is in good agreement with those taken from NMR and X-ray studies.

In the spectrum of ATz the band of 3199 cm^{-1} with a shoulder on the left side was found. This is very typical for amines with N-H···Nhydrogen bonds [50].

Fig.10

The range from 2860 to 2700 cm^{-1} seems to not very useful in assessing the absence of the aldehyde group in the studied Schiff bases. The spectrum of salicylaldehyde (Fig.10, green line) shows two bands in this region: 2846 and 2751 cm^{-1}, which confirms the presence of aldehyde group in investigated compound. However, in the same region there are bands (Fig.10 red line, 2837-2712 cm^{-1}), which one probably can assign to the stretching vibrations of N-H bonds in the ring of ATz [51-52]. This situation makes it very difficult to unambiguously state that there is no unreacted aldehyde in the product.

The next range (1700-1450 cm^{-1}) is always considered during analysis of Schiff bases structures. It is very useful for study of:

i) presence of various intensity bands caused by stretching vibrations of C=N bonds (1645-1592 cm^{-1} for Ar-CH=N-ATz [53-57],

ii) presence of various intensity bands of stretching vibrations of C=O bond in o-hydroxy aromatic Schiff bases occurring in keto form with HB (C=O···H-N) (bands at higher wavenumbers), and C=N bond in enol form with HB (O-H···N=C) (bands at lower wavenumbers) [58] (Fig.11),

iii) absence of strong intensity bands of stretching vibrations of C=O bond connected directly with phenyl in the region 1700-1660 cm^{-1} for benzaldehydes [22],

iiii) absence of strong intensity bands of stretching vibrations of C=O bond in o-hydroxy aldehydes occurring in keto form (doublet in the range from 1730 to 1695 cm^{-1}), and in enol form (one band observed in the region 1640-1570 cm^{-1}) [22] (Fig.11).

Fig. 11

Fig. 11 presents fragment of spectra of aldehyde and its imine derivative. In the 5-bromosalicylaldehyde spectrum (Fig.11 red line) there are three bands in the region characteristic for stretching vibrations of C=O in aldehydes existed in two forms: keto form (1670 and 1651 cm^{-1}) and enol form (1610 cm^{-1}). The last band is probably a result of combination of two vibrations: ν(C=O) of enol form of aldehyde and ν(C=C) of aromatic ring.

In the discussed range of ATR-FTIR spectra of ATz-based Schiff base products there are bands assigned as follows:

1. C=N stretching vibrations (*ν(C=N)*) of the Schiff bases without intramolecular hydrogen bonds (1597-1585 cm^{-1}) (Table 6),
2. stretching vibrations of C=N bond in enol-imine form or C=O bond in keto-amine form of the Schiff bases having intramolecular hydrogen bonds (1639-1602 cm^{-1}) (Table 6).

It is known that IR spectra of heterocyclic Schiff bases without intramolecular hydrogen bonds have typical bands near 1600 cm^{-1} assigned to stretching vibrations of C=N bonds. Spectra of all considered p-substituted benzaldehyde derivatives have two bands in this region (weak or medium at 1618-1613 cm^{-1} and medium or strong at 1597-1585 cm^{-1}). This may be due to possible polymorphic forms existence or due to possible intermolecular hydrogen bonds involving imine group and nitrogen atom in the ring (see NMR and X-ray consideration), or because of the type of substitution in the phenyl ring (according to the Bellamy [50] di-substituted (in *para* position) aromatic compounds influence the shifting of band assigned to ν (C=C) towards higher frequencies).

Table 6 presents wavenumbers of bands which one can assign to:

a) stretching vibrations of **C=N**···H-O in enol-imine form (lower wavenumber) and **C=O**···H-N in keto-amine form (higher wavenumber) bonds in the proton transfer forms of o-hydroxy aromatic Schiff bases,

b) stretching vibrations of C=N bond engaged (higher wavenumbers) or not engaged (lower wavenumbers) in the intermolecular hydrogen bond in the spectra of Schiff bases derived from p-substituted benzaldehydes,

c) comparison of results with the wavenumbers of these bands in the literature (KBr pellet method).

Table 6

As we know from CPMAS NMR study, o-hydroxy aromatic Schiff bases obtained from ATz exist in the solid state as a tautomeric equilibrium of two containing intramolecular hydroden bonds forms: enol-imine and keto-amine, where the first of them is the dominant one (Table 3). The bands assigned to ν(C=N) are shifted to higher wavenumbers comparing with compounds without intramolecular H-bonds.

In some cases two separated bands were found: first close to 1600 cm^{-1} and the second at 1639-1624 cm^{-1}. According to the rule that for o-hydroxy Schiff bases two bands appear in this region of IR spectra: the band in higher wavenumbers (1639-1624 cm^{-1}) for imine existed in the keto-amine form (C=O···H−N), and the band inlower wavenumbers (close to 1600 cm^{-1}) for imine existed in the enol-imine form (C-O-H···N) (Fig.12.) [58], some estimation of contents of tautomeric equilibrium was done and compared with CPMAS NMR data (Table 7). This estimation was done by means of intensity of transmittance of proper bands.

Fig. 12.

It is well visible relation between tautomeric form contents with nitrogen chemical shifts of imine atoms. Higher content of keto-amine form is connected with upfield shift of imine atom, which is in agreement with literature data [43].

Table 7

4. UV-Vis spectroscopy

In the case of heterocyclic molecules, their electronic spectra are usually complex because of combinations of $\pi\rightarrow\pi^*$ and $n\rightarrow\pi^*$ transitions. The common method of studying derivatives of heterocyclic molecules is to compare their spectra to the spectra of the parent heterocyclic systems [22].

The electronic absorption spectra of the ATz-based Schiff bases were recorded in three organic solvents of different polarities (chloroform, acetonitrile, and dimethyl sulfoxide), and in the solid state.

In the UV-Vis spectra recorded during measurements in the solution, bands around 200-300 nm are usually of strong intensity with values of molar absorption coefficients going as high as 10^4 $dm^3 \cdot mol^{-1} \cdot cm^{-1}$. This is indicative of $\pi\rightarrow\pi^*$ electronic transition characteristics of the aromatic system [59].

The two long-wavelength bands, which are correlated with the presence of tautomeric equilibrium of o-hydroxy aromatic Schiff bases (OH-form bands and NH-form bands) in the literature are defined as the CT electronic transitions [56, 60] (Fig. 13). Unfortunately, in some spectra (Table 8, "□") of investigated derivatives the OH-form bands are overlapped with $\pi\rightarrow\pi^*$ of C=C and C=N transitions making exact analyses more complicated.

Fig. 13

Table 8 lists the λ_{max} and ε_{max} values of $\pi\rightarrow\pi^*$ C=C, and C=N, and CT electronic transitions of the studied Schiff's bases.

Table 8

In the case of o-hydroxy aromatic Schiff bases studied in this work, the correlation between polarity of the solvent used and CT band position is visible very well. The increase of solvent polarity causes the hipsochromic shift of this band. It is typical for the compounds which are polar in the ground state [62]. Additionally, for some compounds (4BrsalATz, $4OCH_3$salATz, $3NO_2$salATz, and $5NO_2$salATz), increase in polarity of solvent generates a new, low intensity band, assigned to NH-form. Since the molar extinction coefficient for pure NH form of imine derivatives of ATz is unknown, we were not able to perform the quantitative analysis and could only estimate percentage of tautomeric forms considering

molar integral intensities (Table 8). In these compounds the small integral intensity of NH-form band indicates the equilibrium between two forms OH and NH, which is strongly shifted to OH form. This conclusion is only partly consistent with NMR data, but we have to remember that, apart from mentioned above reason, the concentrations of the samples for both measurements methods are significantly different, which can influence different tautomeric equilibria positions.

On the base of literature data concerning Schiff base structure investigation in the solution, one can assume that in UV-Vis-DR spectra the bands above 400 nm should be assigned to keto-amine form and those below 400 nm to enol-imine tautomer. Unfortunately, the problem is more complicated, since in the electronic spectra in the solid state the pattern of overlapping bands was observed. Anyway, some correlation between position of the band below 400 nm (Fig. 14) and positions of tautomeric equilibria taken from mentioned above spectral methods were found (Table 9). Generally, for the compounds with the same substituent in different positions in phenyl ring, the upfield shift of nitrogen signal of formally imine signal is correlated with CT band shift to higher wavelengths.

Fig.14

For the 3Brsal derivative we could not properly assign the chemical shift of imine nitrogen atom (see NMR consideration) because of signal overlapping with signals of nitrogen atoms in triazolyl ring. Now, comparing with UV-Vis-DR data we can assume, that this signal should be found close to -123 ppm value.

Table 9

Conclusions

Twelve ATz-based Schiff bases were synthesized and analyzed by various analytical techniques (NMR, X-ray, IR, UV-Vis) in the solution and in the solid state. First of all we verified the structure of 3-amino-1,2,4-triazole in the solid state. In DMSO-d6 solution this compound is known as tautomeric mixture of three species. In the solid state only one structure with proton on nitrogen atom N-2' was found. The structure of triazolyl ring in investigated Schiff bases was defined by analysis of ^{13}C and ^{15}N NMR data. Unfortunately, due to tautomeric processes in DMSO-d6 solutions we could not detect any nitrogen signals from this part of molecules, but comparison of carbon signals suggest that in both phases the same structure is present. The crystal structures of two imines confirm that proton in triazolyl ring is located in position N-1'. Analyzing the combined spectroscopic data we found out that in all imines derived from various salicylaldehydes the enol-imine form is the dominant one.

The position of proton in intramolecular hydrogen bridge only in some extend depends on substituent in phenyl ring, which is in contract to Schiff bases obtained from aliphatic amines. In the solid state the tautomeric equilibria of investigated o-hydroxy Schiff bases are shifted to keto-amine form. This effect was observed in aliphatic Schiff bases but again in ATz-based imines it is much weaker. Even application of 5-nitrosalicylaldehyde, which is known to shift strongly tautomeric equilibrium to keto-amine form in the case of ATz derivatives it does not work. To determine the position of tautomeric equilibria the nitrogen chemical shifts of imine atoms seems to be the best choice. In some cases, where no signal overlapping takes place, the IR and UV-Vis data can be valuable source of quantitative estimation.

This work was partly supported by the National Science Centre (No. 2017/01/X/ST4/01132).

References

1. Z. Abbasi, M. Salehi, A. Khaleghian, M. Kubicki *J. Mol. Struct.* 1173 (2018) 213-220

2. P. Dominiak, E. Grech, G. Barr, S. Teat, P. Mallinson, K. Woźniak *Chem. Eur. J.* 9 (2003) 963-970

3. A. Bartyzel, A.A. Kaczor *Polyhedron* 139 (2018) 271-281

4. V.S. Wakale, S.R. Pattan, T. Vishal *Int. J. Res. Pharm. Biomed. Sci.* 4 (2013) 985-1001

5. A. Vlad, M. Avadanei, S. Shova, M. Cazacu, M.-F. Zaltariov *Polyhedron* 146 (2018) 129-135

6. E. Tas, I. Ucar, V.T. Kasumov, A. Kilic, A. Bulut *Spectrochim. Acta Part A* 68 (2007) 463-468

7. P. Zhong-Hua, Z. Jing-Wei, L. Geng-Geng *Phys. Chem. Chem. Phys.* 16 (2014) 16290-16301

8. E. Ermiş *J. Mol. Struct.* 1156 (2018) 91-104

9. Z. Bouhidel, A. Cherouana, P. Durand, A. Doudouh, F. Morini, B. Guillot, S. Dahaoui *Inorg. Chim. Acta* 482 (2018) 34-47

10. F.A. Al-Saif, K.A. Alibrahim, E.H. Alosaimi, E. Assirey, M.S. El-Shahawi, M.S. Refat *J. Mol. Liq.* 266 (2018) 242-251

11. W. Xu, W. Wang, J. Li, Q. Wu, Y. Zhao, H. Hou, Y. Song *Dyes and Pigments* 160 (2019) 1-8

12. G. Wojciechowski, P. Przybylski, W. Schilf, B. Kamieński, B. Brzeziński *J. Mol. Struct.* 649 (2003) 197-205

13. R.M. Issa, A.M. Khedr, H.F. Rizk Spectrochim. Acta Part A 62 (2005) 621-629

14. A. Jamshidvand, M. Sahihi, V. Mirkhani, M. Moghadam, I. Mohammadpoor-Baltork, S. Tangestaninejad, H.A. Rudbari, H. Kargar, R. Keshavarzi, S. Gahraghani *J. Mol. Liq.* 253 (2018) 61-71

15. P. Przybylski, M. Ratajczak-Sitarz, A. Katrusiak, W. Schilf, G. Wojciechowski, B. Brzeziński *J. Mol. Struct.* 655 (2003) 293-300

16. B. Jarząbek, B. Kaczmarczyk, D. Sęk *Spectrochim. Acta Part A* 74 (2009) 949-954

17. A. Makal, W. Schilf, B. Kamieński, A. Szady-Chełmieniecka, E. Grech, K. Woźniak *Dalton Trans.* 40 (2011) 421-430

18. W. Schilf, B. Kołodziej, E. Grech *J. Mol. Struct.* 791 (2006) 93-97

19. W. Schilf, B. Kamieński, A. Szady-Chełmieniecka, B. Kołodziej, E. Grech, D. Zarzeczańska, A. Wcisło, T. Ossowski *Spectrochim. Acta Part A: Mol. Biomol. Spectrosc.* 109 (2013) 47-54

20. A. Szady-Chełmieniecka, B. Kołodziej, M. Morawiak, B. Kamieński, W. Schilf *Spectrochim. Acta Part A: Mol. Biomol. Spectrosc.* 189 (2018) 330-341

21. B. Kołodziej, P.M. Dominiak, A. Kościelecka, W. Schilf, E. Grech, K. Woźniak *J. Mol. Struct.* 691 (2004) 133-139

22. W. Schilf, B. Kamieński, K. Užarevič *J. Mol. Struct.* 1031 (2013) 211-215

23. R.M. Issa, K.Y. El-baradie, N.A. El-Wakiel *Spectrochim. Acta Part A* 60 (2004) 2883-2889

24. D.L. Pavia, G.M. Lampman, G.S. Kriz, J.R. Vyvyan *Introduction to Spectroscopy* 2015(published by Brooks/Cole, Cengage Learning in 2009)

25. K. Ambroziak, Z. Rozwadowski, T. Dziembowska, B. Bieg *J. Mol. Struct.* 615 (2002) 109-120

26. K. Görgün, H.C. Sakarya, M. Ozkütük *J. Chem. Eng. Data* 60 (2015) 594-601

27. V.I. Minkin, A.V. Tsukanov, A.D. Dubonosov, V.A. Bren *J. Mol. Struct.* 998 (2011) 179-191

28. L.R. Knöpke, S. Reimann, A. Spannenberg, P. Langer, A. Brückner, U. Bentrup *Monatsch. Chem.* 144 (2013) 421-428

29. L. Wang, Y. Li, X. You, K. Xu, Q. Feng, J. Wang, Y. Liu, K. Li, H. Hou *J. Mater. Chem. C* 5 (2017) 6572

30. A.K. Wahi, A. Singh Asian *J. Biochem. Pharm. Res.* 1 (2011) 193-205

31. Q.J. Zhao, Y. Song, H.G. Hu, S.C. Yu, Q.Y. Wu *Chin. Chem. Lett.* 18 (2007) 670-672

32. S.E. Glynn, P.J. Baker, S.E. Sedelnikova, C.L. Davies, T.C. Eadsford, C.W. Levy, H.F. Rodgers, G.M. Blackburn, T.R. Hawkes, R. Viner, D.W. Rice *Structure* 13 (2005) 1809-1817

33. T.K. Chaitra, K.N.S. Mohana, H.C. Tandon *J. Mol. Liq.* 211 (2015) 1026-1038

34. P.P. Utthra, G. Kumaravel, N. Raman *J. Mol. Struct.* 1150 (2017) 374-382

35. Bruker, 2004, APEX2 and SAINT. Bruker AXS Inc., Madison, Wisconsin, USA

36. G. M. Sheldrick, Acta Crystallogr., Sect. A: Found. *Crystallogr.*, 2008,64, 112.

37. Bruker, 2008, SADABS. Bruker AXS Inc., Madison, Wisconsin, USA.

38. G. M. Sheldrick, SHELXL-2014. *Program for the Refinement of Crystal Structures from Diffraction Data*, University of Göttingen, Germany (2014).

39. H. Fritz, *Bull. SOC. Chim. Belg.*, 93 (1984) 559

40. M. Witanowski, L. Stefaniak, G.A. Webb, *Annual Reports on NMR Spectroscopy*, vol. 25, Academic Press , London, 1993

41. W.Schilf, J.P.Bloxsidge, J.R. Jones, S.-Y. Lu, *Mag. Reson. Chem.* 42 (2004) 556

42. W. Schilf, B. Kamieński, A.Szady-Chełmieniecka, E. Grech, *Solid State NMR* 18 (2000) 97

43. B. Kamieński, W.Schilf, T. Dziembowska, Z. Rozwadowski, A. Szady-Chełmieniecka, *Solid State NMR*, 16 (2000) 285

44. W. Schilf, B. Kamieński, T. Dziembowska, *J. Mol. Struct.*, 602-603 (2002) 41

45. W. Schilf, B. Kamieński, A. Szady-Chełmieniecka, E. Grech, *J. Mol. Struct.* 700 (2004) 105

46. W. Schilf, B. Kamieński and T. Dziembowska, Z.Rozwadowski, A. Szady-Chełmieniecka, *J. Mol. Struct.*, 552 (2000) 33

47. W. Schilf, B. Kamieński, B. Kołodziej, E. Grech, *J. Mol. Struct.*, 708 (2004) 33

48. Z.H. Chochan, M. Hanif *Appl. Organometal. Chem.* 25 (2011) 753-760

49. R.M. Issa, A.M. Khedr, H.F. Rizk *J. Chin. Chem. Soc.* 55 (2008) 875-884

50. L.J. Bellamy *The Infra-red Spectra of Complex Molecules* London 1962

51. S.G. Aziz, S.A. Elroby, A. Alyoubi, O.I. Osman, R. Hilal *J. Mol. Model.* 20 (2014) 2078-2093

52. D. Bougeard, N. Le Calve, B. Saint Roch, A. Novak *J. Chem. Phys.* 64 (1976) 5152-5164

53. S.H. Sumrra, A. Suleman, Z.H. Chochan, M.N. Zafar, M.A. Raza, T. Iqbal *Russ. J. Gen. Chem.* 87 (2017) 1281-1287

54. M.M. Ayad, I.A. Mansour *Monatsch. Chem.* 126 (1995) 385-392

55. P.P.Utthra, N. Pravin, N. Raman *J. Photochem. Photobiol. B* 158 (2016) 136-144

56. Y.M. Issa, H.B. Hassib, H.E. Abdelaal, I.M. Kenawi *Spectrochim. Acta Part A* 79 (2011) 1364-1374

57. B. Liu, T.-Y. Yang, H.-J. Feng, Z.-H. Zhang, L. Xu *J. Solid State Chem.* 230 (2015) 90-94

58. I. Majerz, A. Pawlukojć, L. Sobczyk, T. Dziembowska, E. Grech, A. Szady-Chełmieniecka *J.Mol.Struct.* 552 (2000) 243-247

59. H.-H. Tang, L. Zhang, L.-L. Zeng, X.-M. Fang, L.-R. Lin, H. Zhang *RSC Adv.* 5 (2015) 36813-36819

60. Vanco_2010. J. Vančo, Z. Trávníček, J. Marek, R. Herchel *Inorg. Chim. Acta* 363 (2010) 3887-3896

61. El-Haty1990. A. El-Haty, M. Gabr *J. Indian Chem. Soc.* 67 (1990) 743-747

62. C.N.R. Rao *Ultra-Violet and Visible Spectroscopy. Chemical Applications*, London 1975

Table 2. Results of NMR measurements in DMSO solution.

		1	2	3	4	5	6	7	N-**H**	O-**H**	N_{im}	5'	3'	OCH_3
4BrbenzATz	^{1}H	-	7.92	7.72	-	7.72	7.92	9.18	14.0 320Hz	-	-	8.33 27Hz	-	-
	$^{13}C/^{15}N$	134.9	131.4	132.5	126.5	132.5	131.4	163.3		-	-82.1#	146 300Hz	**	-
4OCH_3benzATz	^{1}H	-	7.93	7.07	-	7.07	7.93	9.11	13.9 30Hz	-	-	8.40 120Hz		3.82
	$^{13}C/^{15}N$	128.8	131.6	115.0	163.2	115.0	131.6	163.1		-	no signal	143.7 50Hz	166.3 50Hz	56.0
4NO_2benzATz	^{1}H	-	8.23	8.33	-	8.33	8.23	9.32	14.1 50 Hz	-	-	8.52 80 Hz	-	-
	$^{13}C/^{15}N$	141.4	130.6	124.6	149.6	124.6	130.6	161.7		-	-69.6	144.7 13Hz	166.1 12Hz	-
salATz	^{1}H	-	-	6.96 ov.	7.42	6.96 ov.	7.77	9.43	14.1 300Hz	12.4 270Hz	-	8.44 58Hz	-	-
	$^{13}C/^{15}N$	119.7	160.8	117.3*	134.8	119.9*	132.8	165.3			-107.6	146.0 170Hz	163.0 200Hz	-
3BrsalATz	^{1}H	-	-	-	7.75	6.95	7.79	9.40	14.20 76Hz	13.88 120Hz	-	8.57 60Hz		-
	$^{13}C/^{15}N$	110.7	157.6	120.5	137.3	121.1	133.7	165.9			-110.0	145.0 10Hz	163.7 9Hz	-
4BrsalATz	^{1}H	-	-	7.19	-	7.15	7.75	9.39	14.1 40Hz	12.67 110Hz	-	8.53 80Hz	-	-
	$^{13}C/^{15}N$	127.7	161.3	120.0	119.3	123.2	133.7	163.9			-103.6	144.8 24Hz	164.6 24Hz	-
5BrsalATz	^{1}H	-	-	6.97	7.59	-	8.04	9.42	14.16 53Hz	12.4 120Hz	-	8.55 90Hz	-	-
	$^{13}C/^{15}N$	121.9	159.7	119.7	136.8	110.9	133.8	163.2			-100.2	144.8 17Hz	164.7 12Hz	-
3OCH_3salATz	^{1}H	-	-	-	7.14	6.90	7.37	9.39	14.1 130Hz	12.4 220Hz	-	8.43 74Hz	-	3.80
	$^{13}C/^{15}N$	119.6	150.9	148.4	116.6	119.5	123.9	165.5			-107.4	145.3 200Hz	163.8 300Hz	56.3
4OCH_3salATz	^{1}H	-	-	6.50	-	6.55	7.65	9.27	13.98 50Hz	13.12 110Hz	-	8.5 90Hz	-	3.79
	$^{13}C/^{15}N$	113.1	163.5	101.4	164.8	107.9	134.8	165.0			-120.2	144.6 90Hz	164.9 30Hz	56.1
5OCH_3salATz	^{1}H	-	-	6.90	7.04	-	7.37	9.40	14.07 54Hz	11.72 140Hz	-	8.43 100Hz	-	3.72
	$^{13}C/^{15}N$	119.7	155.0	118.2	122.2	152.6	114.4	164.5			-103.2	144.2 30Hz	164.0 40Hz	56.0
3NO_2ATz	^{1}H	-	-	-	8.12	7.14	8.15	9.50	14.25 19Hz	14.4 v.br	-	8.63 11 Hz	-	-
	$^{13}C/^{15}N$	121.9	155.4	139.4	130.0	119.4	138.9	164.9			-109.6	145.6 32Hz	163.3 38Hz	-
5NO_2salATz	^{1}H	-	-	7.14	8.25	-	8.79	9.51	14.2 52Hz	13.0 390Hz	-	8.57 56Hz	-	-
	$^{13}C/^{15}N$	120.3	165.7	118.3	129.3	140.5	127.2	162.0			-97.2	145.0 90Hz	164.5 100Hz	-
ATz	^{1}H	-	-	-	-	-	-	-	11.9 80% 12.7 20%	-	-	7.29 80% 7.96 20%	-	-
	$^{13}C/^{15}N$	-	-	-	-	-	-	-		-	-	149.2 80% 141.9 20%	156.4 80% 163.8 20%	-

*-assignment can be changed
**-probably very broad signal close to 163 ppm overlapped with C-7 signal
#-value measured at 80℃
ov. – overlapped signals
for ATz chemical shift of nitrogen atom of NH is -203.3 ppm

Table 3. Nitrogen and carbon chemical shifts of selected salicylaldehyde derivatives in solid state from CPMAS experiments.

	C-1	C-2	C-3	C-4	C-5	C-6	C-7	C-3'	C-5'	N_{im}	N-1' (NH)	N-2'	N-4'	NO_2	CH_3
3BrsalATz	106.0 v.broad	162.6	118.9	137.4 broad	120.8	131.1 134.1	161.7	157.7	144.4	-117.7$ -122.0$ -123.3$	-172.6 -170.2 -168.4	-110.5$ -114.3$ -116.0$	-152.6 -149.6?		
4BrsalATz	116.8	155.3	119.6	124.9*	124.9*	135.7	163.0	162.9	150.6	-135.2	-174.4	-90.0	-165.4	-	-
5BrsalATz	120.2	159.7	117.2	139.4	111.7 broad	136.0	162.5	161.2	142.5	-121.7	-170.2	-112.7	-151.7		
3OCH_3salATz	117.5	150.9 152.5	147.1 149.7	112.9	116.9	122.0 123.4	162.1 162.7	162.6	142.9 146.2	-115.1% -119.5%	-171.1	-104.7% -112.4%	-153.6	-	56.4
4OCH_3salATz	113.0 116.8	162.4 163.1#	97.3	167.2#	109.7 111.5	135.4 136.9	164.9	156.8	149.3	-147.4 broad	-177.6	-97.4	-167.5	-	54.9
5OCH_3salATz	117.3*	156.4*	117.3*	126.2	151.9	112.7	170.1	156.4*	148.5	-136.6	-175.1 broad	-96.9 -95.3	-167.7 -166.2	-	54.3 56.0
3NO_2salATz	@	157.4 158.3	134.3	129.3 132.7	119.7 121.3	143.5 144.2#	161.8*	161.8*	141.2 143.5#	-119.6 -117.1?	-176.8 -169.2	-100.8?	-162.3 -153.7	-12.8 -8.1	-
5NO_2salATz	117.3	163.3#	121.3	129.3*	139.6	129.3*	163.3	165.4#	145.1	-108.7*	-173.2	-108.7*	-153.6	-11.3	-
ATz	-	-	-	-	-	-	-	156.6	147.9	NH_2 -325.7	-206.0	-116.7	-176.5		

@-quaternary C-1 signal completely overlapped by C-5 signals
%-four close signals, no arguments to distinguish them
*- overlapped signals
#- assignment can be reversed
$-six close signals, no arguments to assign them properly

Table 5. Hydrogen bond distances (Å) and angles (°).

D-H ···A	D-H	H···A	D···A	Angle	Symmetry codes
4BrbenzATz					
N3–H1···N1	0.78(5)	2.20(5)	2.961(4)	167(5)	[x + 1/2, -y + 3/2, z – 1/2]
C9–H9···N4	0.92(5)	2.53(4)	3.176(5)	127(3)	
4BrsalATz					
O1–H2···N1	0.99(6)	1.74(6)	2.592(2)	143(5)	
C5–H5···Br1	1.06(5)	3.03(5)	3.187(4)	131(3)	[-x + 2, -y, z – 1/2]
C9–H9···O1	0.93	2.43	3.283(5)	152.1	[-x + 3/2,y + 1, z – 1/2]

Table 6. Chosen ATR-FTIR spectral data of ATz-based Schiff bases.

Compound	Wavenumber [cm^{-1}]	
	Observed (ATR)	Literature data (KBr)
4BrbenzATz	1613 (m), 1585 (m)[a]	1592 [53]
4OCH_3benzATz	1613 (w), 1597 (s)[a]	1595 [53]; 1601 [56]
4NO_2benzATz	1618 (w), 1595 (m)[a]	1599 [56]; 1605 [53]; 1638 [34]
salATz	1610 (s)	1610 [56]; 1620 [53]; 1636 [52]; 1645 [55]
3BrsalATz	1639 (vw), 1607 (s)[a]	-
4BrsalATz	1624 (w), 1604 (s)[a]	-
5BrsalATz	1611 (s)	1632 [54]
3OCH_3salATz	1611 (s)	1630 [52]
4OCH_3salATz	1639 (m), 1602 (s)[a]	-
5OCH_3salATz	1633 (vw), 1617 (s)[a]	1638 [55]
3NO_2salATz	1620 (s)	-
5NO_2salATz	1615 (m)	1635 [54]; 1643 [55]

s – strong intensity; m – medium intensity; w – weak intensity, vw – very weak intensity

[a] –there are two bands in the range characteristic of bands assigned to ν(C=N).

ATz : band of N-H bending vibrations (primary amino group and N-H bond in the ring) – observed at 1635 (s); found in the literature [57] at 1639 (s). In the spectra of Schiff bases strong bands of C=O and C=N stretching vibrations usually overlap bands assigned to bending vibrations of N-H bond in the ring [58].

Table 7. Estimated percentage of tautomeric forms in o-hydroxy aromatic Schiff bases based on ATz.

Compound	Estimated percentage of tautomeric forms in investigated compounds [%]		δ_{Nim} [ppm] (Table 3)
	Enol-imine form	Keto-amine form	
3BrsalATz	90	10	-110.0 ÷ -123.0
4BrsalATz	78	22	-135.2
5OCH_3salATz	76	24	-136.6
4OCH_3salATz	63	37	-147.4

Table 8. Electronic absorption bands of $\pi \rightarrow \pi^*$ and CT electronic transitions of ATz-based Schiff's bases in various solvents and in the solid state.

Compound	Electron transition	λ_{max} [nm] ($\varepsilon_{max} \cdot 10^4$) [$dm^3 \cdot mol^{-1} \cdot cm^{-1}$]			λ_{max}
		$CHCl_3$	CH_3CN	$(CH_3)_2SO$	DR
4BrbenzATz	$\pi \rightarrow \pi^*$	294.4 ([b])	284.2 ([b])	304.3 (0.53)	358.0
4OCH_3benzATz	$\pi \rightarrow \pi^*$	a	312.5 (2.18)	316.6 (2.42)	370.0
4NO_2benzATz	$\pi \rightarrow \pi^*$	313.9 ([b])[d]	312.0 ([b])	324.3 (1.84)[d]	368.0
salATz	$\pi \rightarrow \pi^*$	□ 300 (□3.10)[c]	□ 300 (□1.30) [c]	□ 300 (□2.80) [c]	□ 335 [c]
	CT	347.4 (1.66)[d]	340.6 (0.97)	341.6 (0.44)[d]	385.5 [c]
3BrsalATz	$\pi \rightarrow \pi^*$	□ 305 (□1.70) [c]	□ 305 (□1.40) [c]	□ 310 (□1.90) [c]	□ 323[c]
	CT	350.8 (0.91)	343.0 (0.81)	342.7 (1.19)	371.0
4BrsalATz	$\pi \rightarrow \pi^*$	303.1 (2.14)	301.3 (2.90)	306.4 (1.84)	□ 323[c]
	CT	345.9 (1.71)	338.3 (2.47)	340.8 (2.10) 98.6% 448.2 (0.029) 1.4%	399.0
5BrsalATz	$\pi \rightarrow \pi^*$	a	□ 305 (□1.00) [c]	□ 310 (□0.80) [c]	□ 315[c]
	CT		351.3 (0.82)	351.6 (0.87)	368.0 □ 490
3OCH_3salATz	$\pi \rightarrow \pi^*$	303.9 (2.10)	□ 300 (□1.00) [c]	305.2 (2.56)	□ 325[c]
	CT	358.4 (0.48)	□ 350 (□0.20) [c]	□ 350 (□0.70) [c]	370.5
4OCH_3salATz	$\pi \rightarrow \pi^*$	a	302.7 (2.12)	307.1 (1.74)	334.0
	CT		338.6 (3.11) □ 405 (□0.039) [c]	341.6 (2.95) 99.2% 497.9 (0.024) 0.8%	385.5
5OCH_3salATz	$\pi \rightarrow \pi^*$	□ 310 (□1.00) [c]	□ 310 (□1.00) [c]	□ 300 (□1.30) [c]	□ 334[c]
	CT	381.7 (0.67)	373.1 (0.71)	374.0 (0.81)	380.5
3NO_2salATz	$\pi \rightarrow \pi^*$	□ 305 (□1.00) [c]	□ 310 (□1.00) [c]	□ 290 (□1.30) [c]	□ 330[c]
	CT	356.0 (0.95)	349.2 (0.96)	346.8 (1.06) 75.8% 477.2 (0.34) 24.2%	388.5
5NO_2salATz	$\pi \rightarrow \pi^*$	283.9 (1.85)	283.7 (2.52)	311.3 (1.32)[c]	□ 336[c]
	CT	327.6 (0.99)	324.9 (1.40)	□ 350 (□0.70) [c] 432.2 (0.66)	377.0

a – insoluble
b – concentration of sample is unknown due to its very low solubility
c – broad band; there are probably few bands which are overlapped each other
d – the literature data for 4NO_2benzATz [61]: 313.0 nm ($CHCl_3$) and 320.0 nm (DMSO), and 304.0 nm (CH_3OH) [56]; for salATz: 348.0 nm ($CHCl_3$), 345.0 nm (DMSO), and 344.0 nm (CH_3OH) (ε_{max} = 1.49) [56]; for 4OCH_3benzATz: 316.0 (CH_3OH) (ε_{max} = 2.4) [56]

Table 9. Comparison of results obtained from ^{15}N NMR measurements with UV-Vis data in the solid state.

Aldehyde part	3Brsal	5Brsal	4Brsal	3OCH_3sal	5OCH_3sal	4OCH_3sal	3NO_2sal	5NO_2sal
^{15}N NMR [ppm]	close to -123.0	-121.0	-135.2	-115.1 -119.5	-136.6	-147.4	-117.1 -119.6	-108.7
UV-Vis-DR [nm]	371.0	368.0	399.0	370.5	380.5	385.5	388.5	377.0

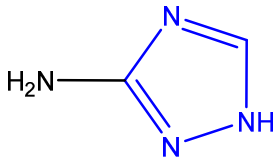

Fig.1. 3-amino-1H-1,2,4-triazole (Amitrole, ATz)

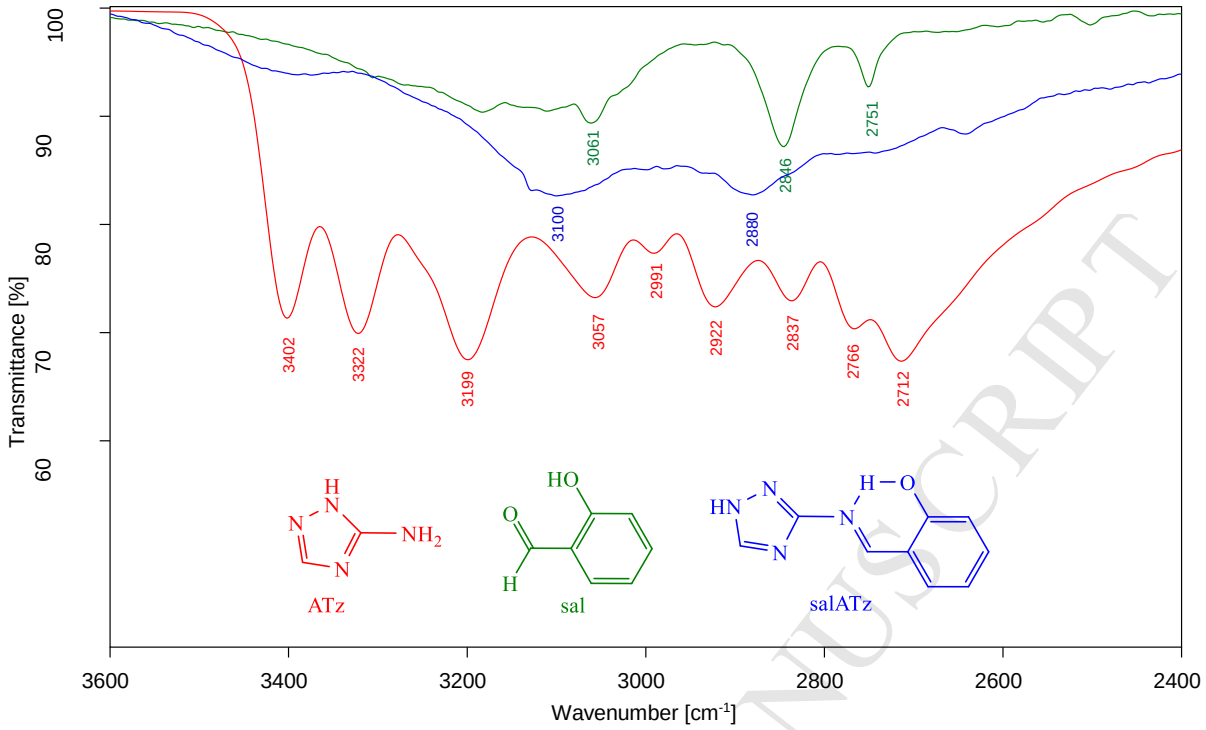

Fig.10. ATR-FTIR spectra of ATz (red line), sal (green line), and salATz (blue line) in the range from 3600 to 2400 cm^{-1}

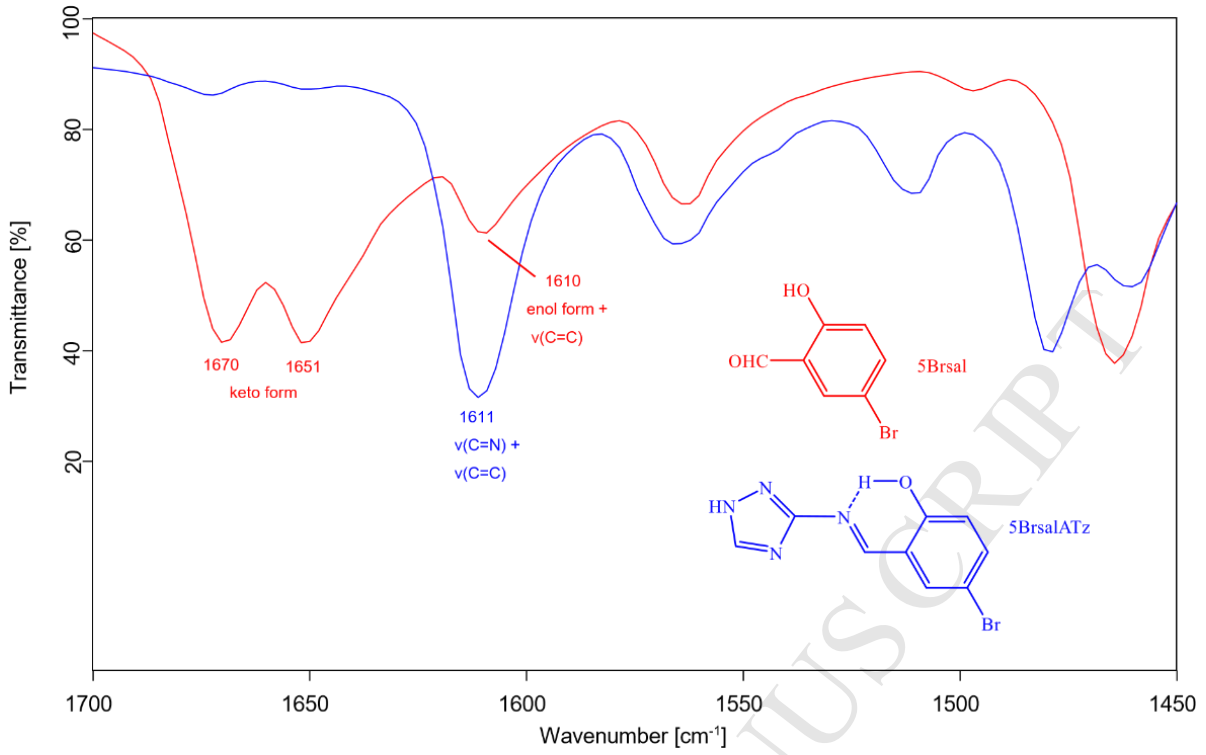

Fig. 11. ATR-FTIR spectra of 5-bromosalicylaldehyde (red line) and Schiff base derived from 5Brsal and ATz (blue line) in the range of 1700-1450 cm^{-1}.

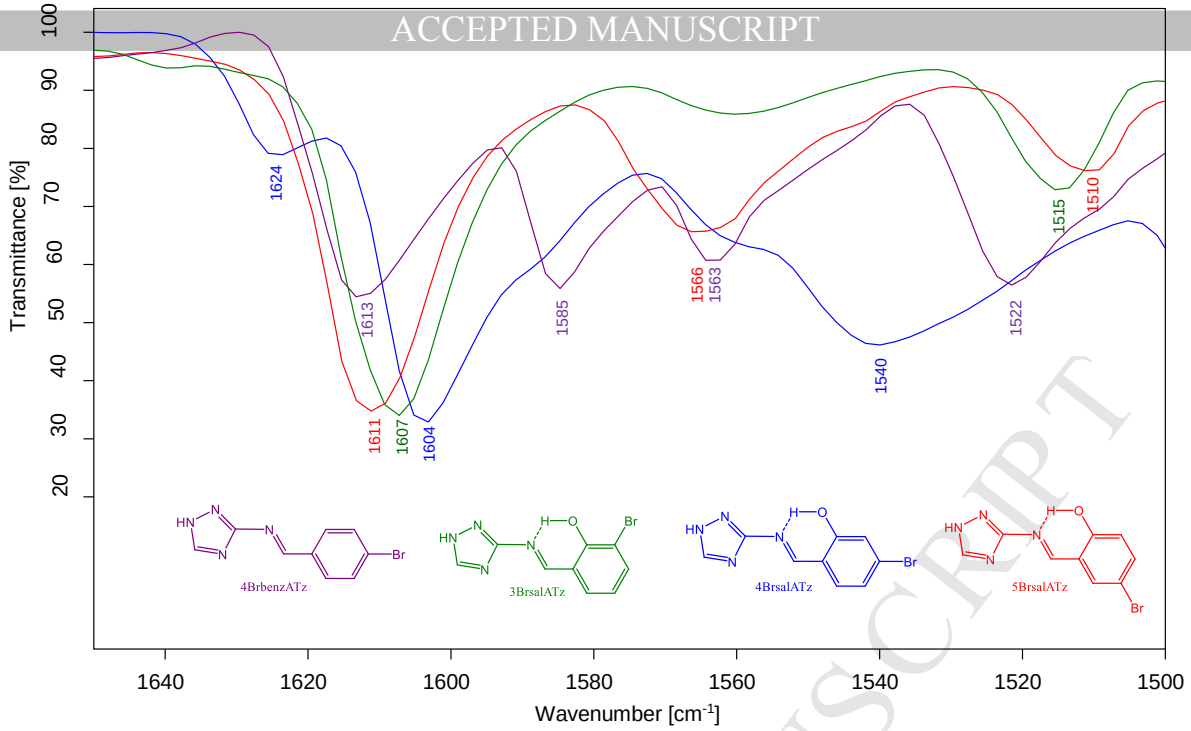

Fig. 12. ATR-FTIR spectra of imine derived from ATz and 4-bromobenzaldehyde (violet line), 3-bromosalicylaldehyde (green line), 4-bromosalicylaldehyde (blue line), and 5-bromosalicylaldehyde (red line) in the range 1650-1500 cm^{-1}.

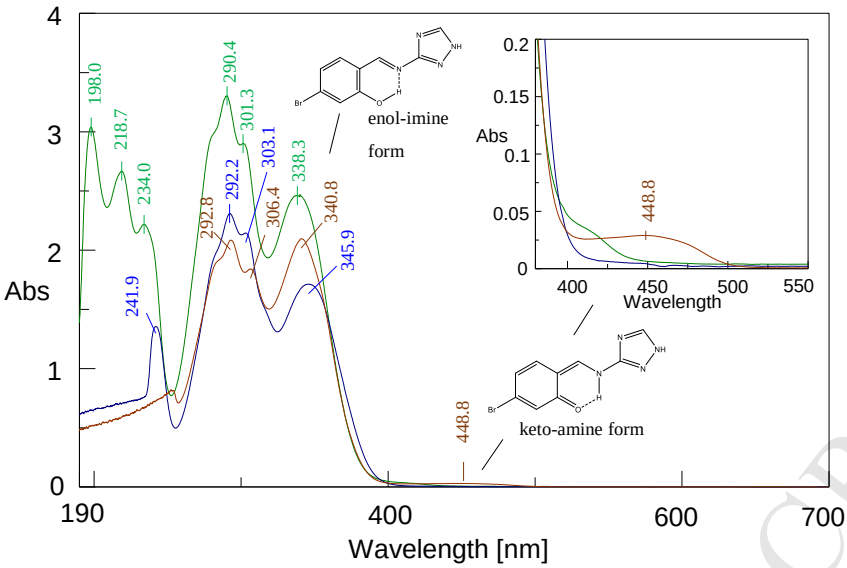

Fig. 13. UV-Vis spectra of 4BrsalATz in $CHCl_3$ (blue line), CH_3CN (green line), $(CH_3)_2SO$ (brown line).

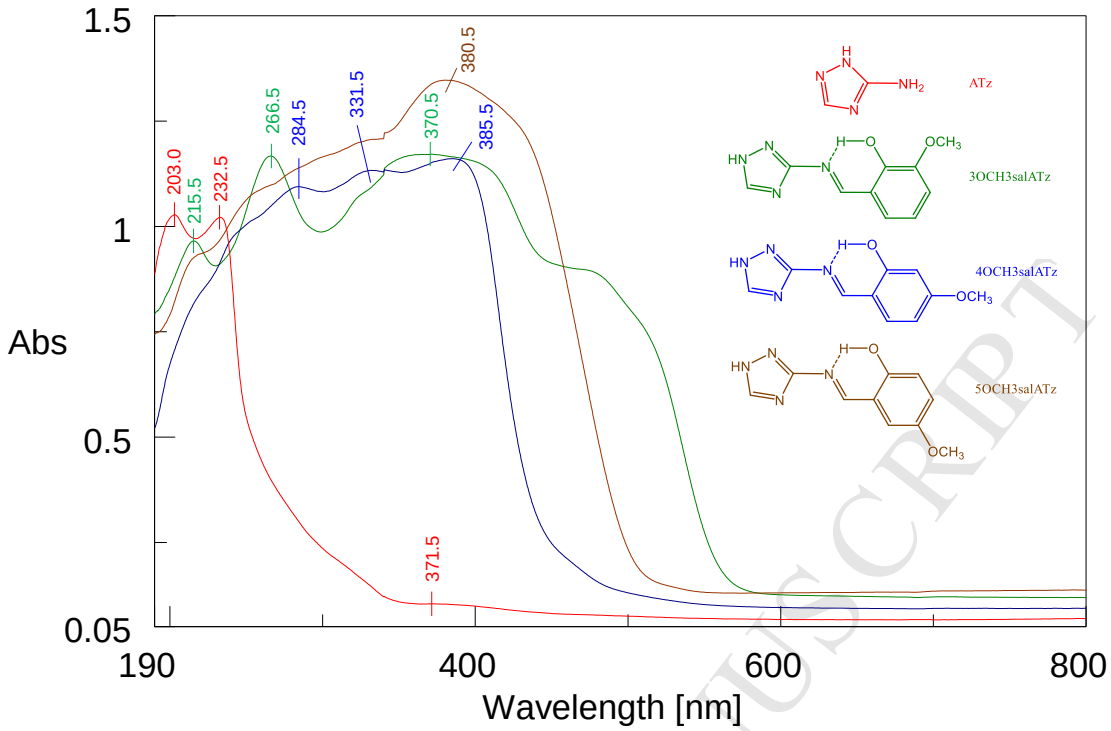

Fig.14. UV-Vis-DR spectra of ATz (red line), 3OCH_3salATz (green line), 4OCH_3salATz (blue line), and 5OCH_3salATz (brown line)

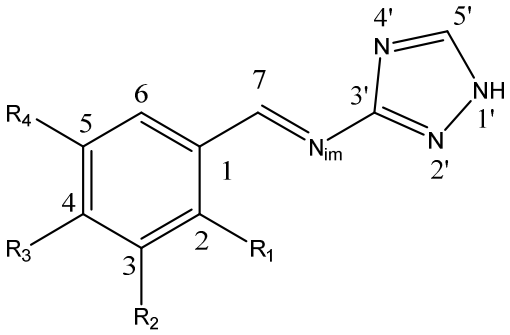

	R1	R2	R3	R4
4BrbenzATz	H	H	Br	H
4OCH_3benzATz	H	H	OCH_3	H
4NO_2benzATz	H	H	NO_2	H
salATz	OH	H	H	H
3BrsalATz	OH	Br	H	H
4BrsalATz*	OH	H	Br	H
5BrsalATz	OH	H	H	Br
3OCH_3salATz	OH	OCH_3	H	H
4OCH_3salATz*	OH	H	OCH_3	H
5OCH_3salATz	OH	H	H	OCH_3
3NO_2salATz*	OH	NO_2	H	H
5NO_2salATz	OH	H	H	NO_2

Fig.2. The general structure and atom numbering in investigated Schiff bases derived from ATz and appropriate aldehydes (* - new compound)

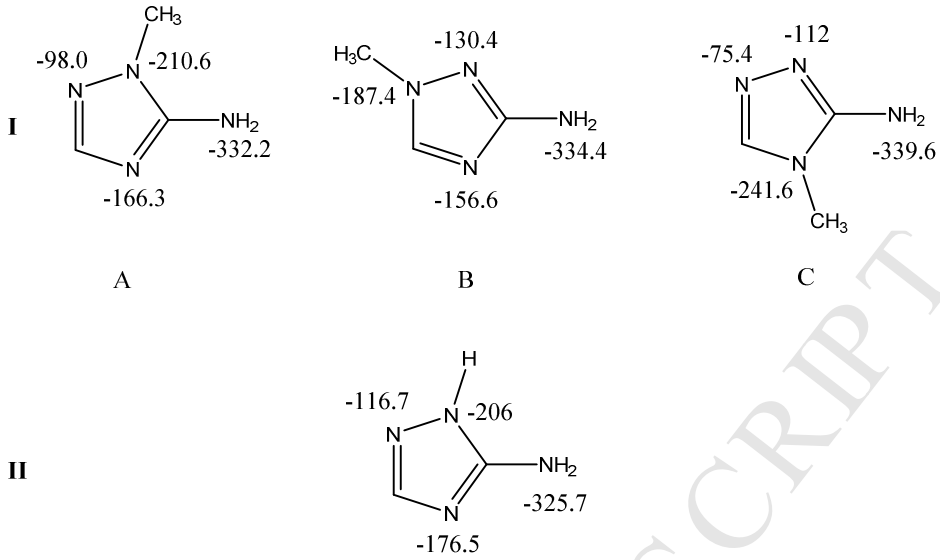

Fig.3. Chemical shifts of nitrogen atoms of methyl derivatives of ATz in DMSO solution (I) and ATz in the solid state (II)

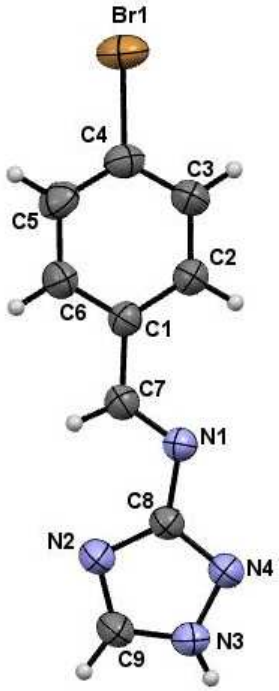

4BrbenzATz

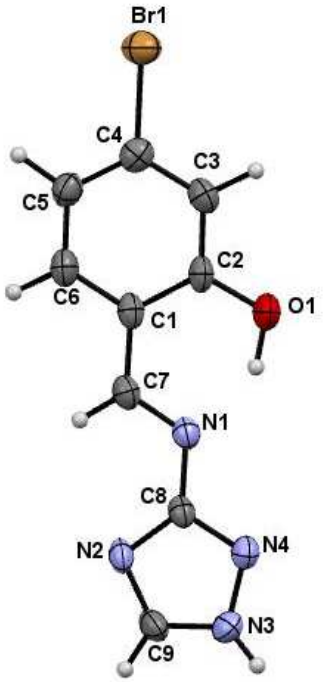

4BrsalATz

Fig.4. A view of the molecules of 4BrbenzATz and 4BrsalATz in conformations observed in their crystals with the atom labelling scheme. Displacement ellipsoids are drawn at the 50% probability level.

Fig.5. Intermolecular hydrogen bonds occurring in 4BrbenzATz.

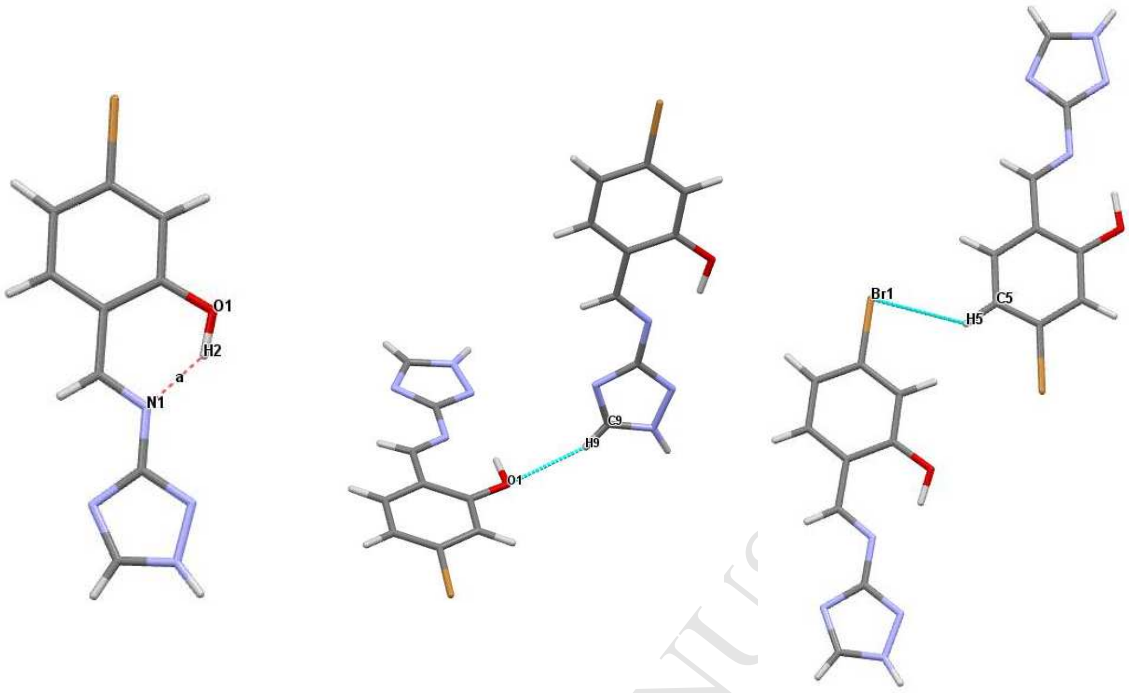

Fig.6. The hydrogen bonds that stabilize the structure of 4BrsalATz.

Highlights

1. Synthesis of twelve 3-amino-1H-1,2,4-triazole (ATz)-based Schiff bases without and with intramolecular hydrogen bond.

2. Spectroscopic analysis of products by X-ray, NMR, ATR-FTIR, and UV-Vis methods.

3. ATz exists as a mixture of three forms (1N-H, 2N-H, and 4N-H) in solution, and as one form (2N-H) in the solid state.

4. Triazole ring in ATz-based Schiff bases exists in 1N-H form in both phases.

5. ATz-salicylaldehydes Schiff bases exist mainly in the enol-imine form.